

## INTRODUCTION

Visual attention improves sensory processing as well as perceptual readout and behavior. How attention shapes cortical signal dynamics across layers, and the interactions between cortical layers within and between visual sensory areas is still just an emerging question [1–3].

## METHODS

We recorded laminar signals from 16 contact silicon probes in V1 and V4 of two macaque monkeys (Figure 1). Animals performed a covert, feature-based spatial attention task (Figure 2).

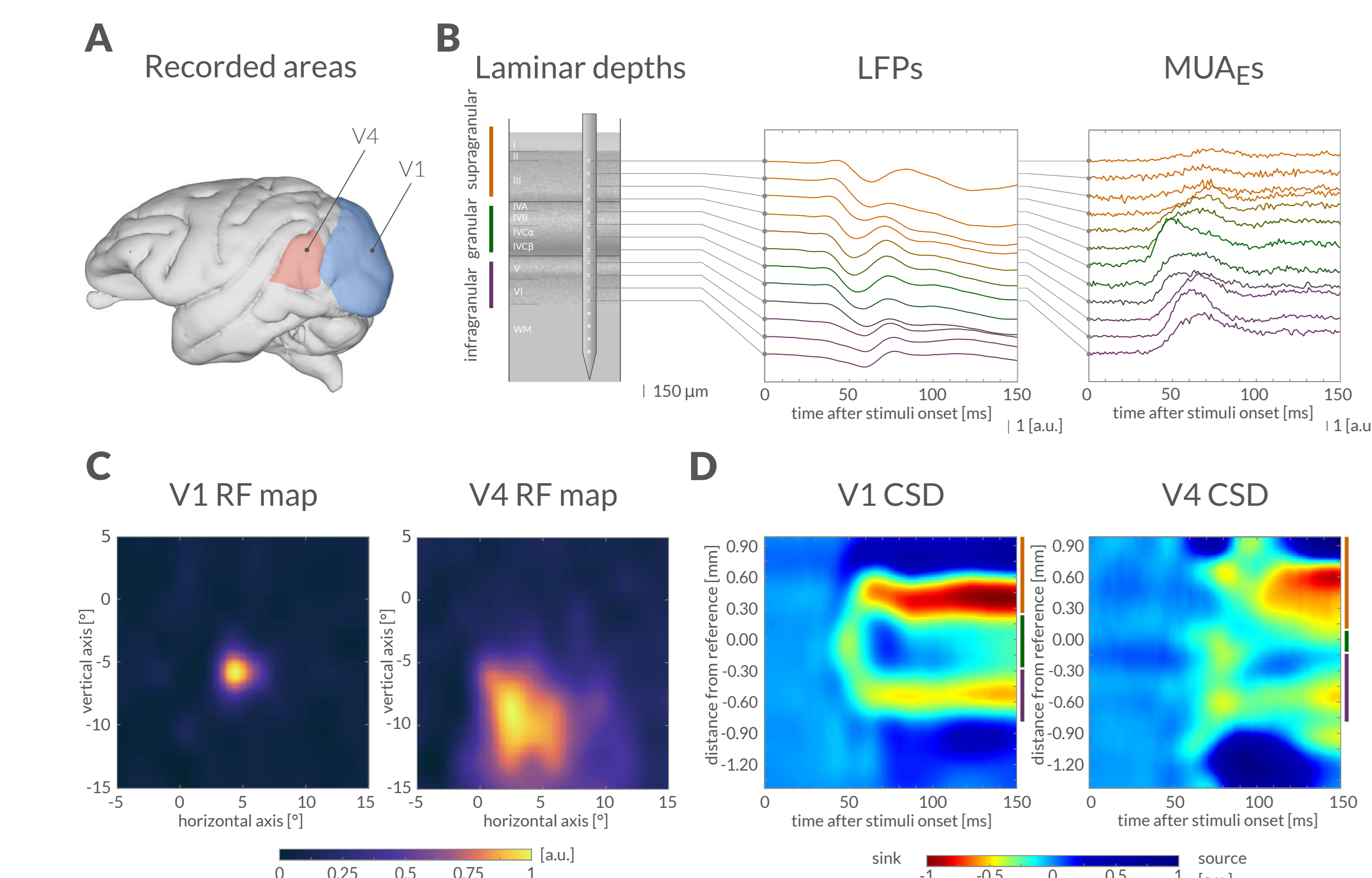
Electrodes were inserted normal to the cortical surface. Recording contacts were aligned to laminar layer IV, identified through current source densities (CSDs) of Local Field Potential (LFP) signals (Figure 1E–F) and latency analysis of multi-unit activity envelopes (MUAEs). We aimed at understanding intra-areal interactions (within V1, within V4) and inter-areal interactions (between V1 and V4). The latter were analysed when recording sites had overlapping receptive fields (RFs, Figure 1C).

The analyses focused on LFP signals, locally re-referenced (bipolar). Spectral power and spectral coherence of LFP signals were computed through multi-taper estimation (using  $K=3$  tapers,  $TW=2$ ).

Directed interactions among LFPs at different laminar depths were analysed using partially conditioned Granger Causality (cGC) [5].

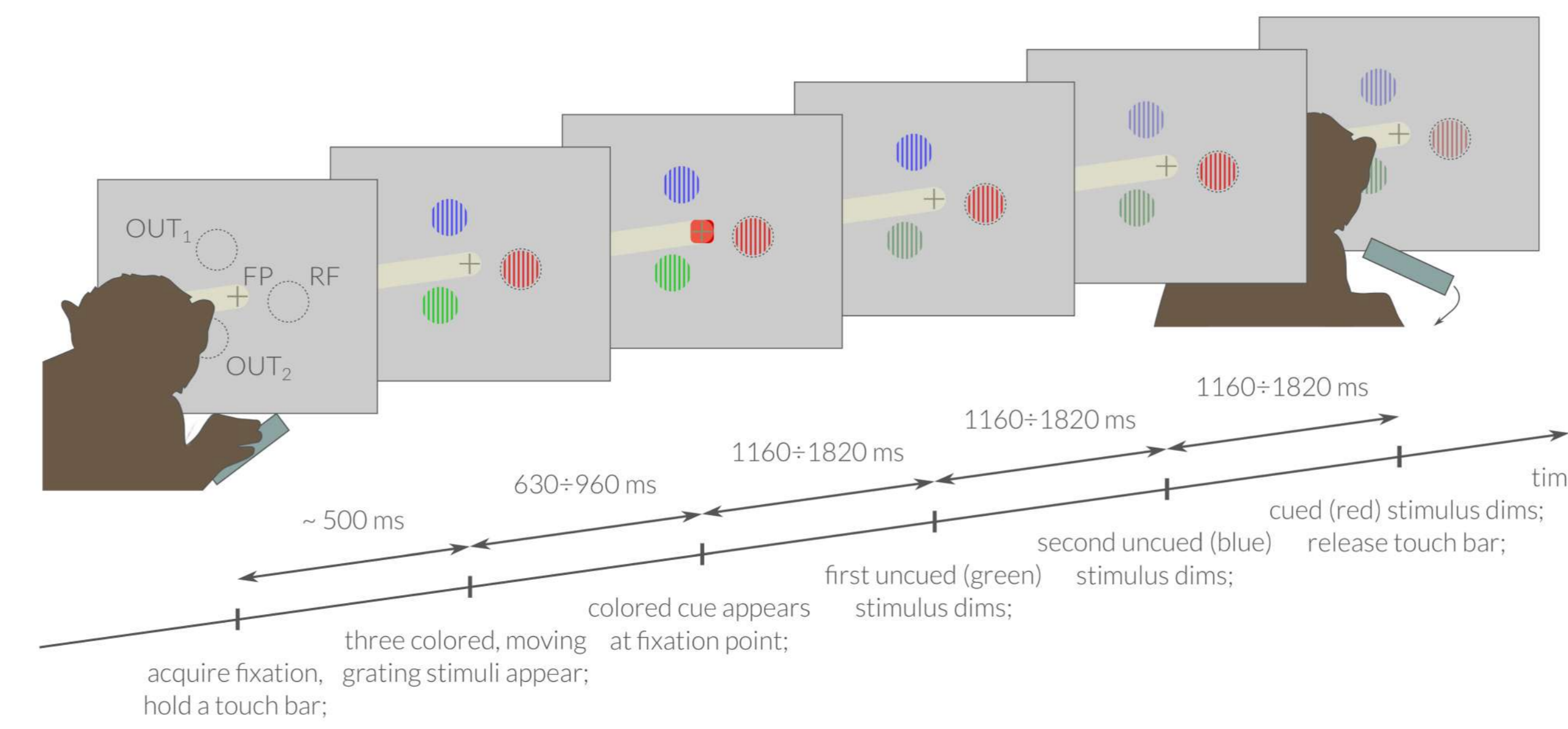
Attentional modulatory effects were determined using a modulation index  $MI = (f_{RF} - f_{OUT}) / (f_{RF} + f_{OUT})$ , where  $f_{RF}$  and  $f_{OUT}$  are estimations of the measure  $f$  (e.g. spectral power, coherence, Granger causal interaction) in task trials where attention was directed inside RF or OUT, respectively.

## Figure 1 – Recording setup and laminar alignment



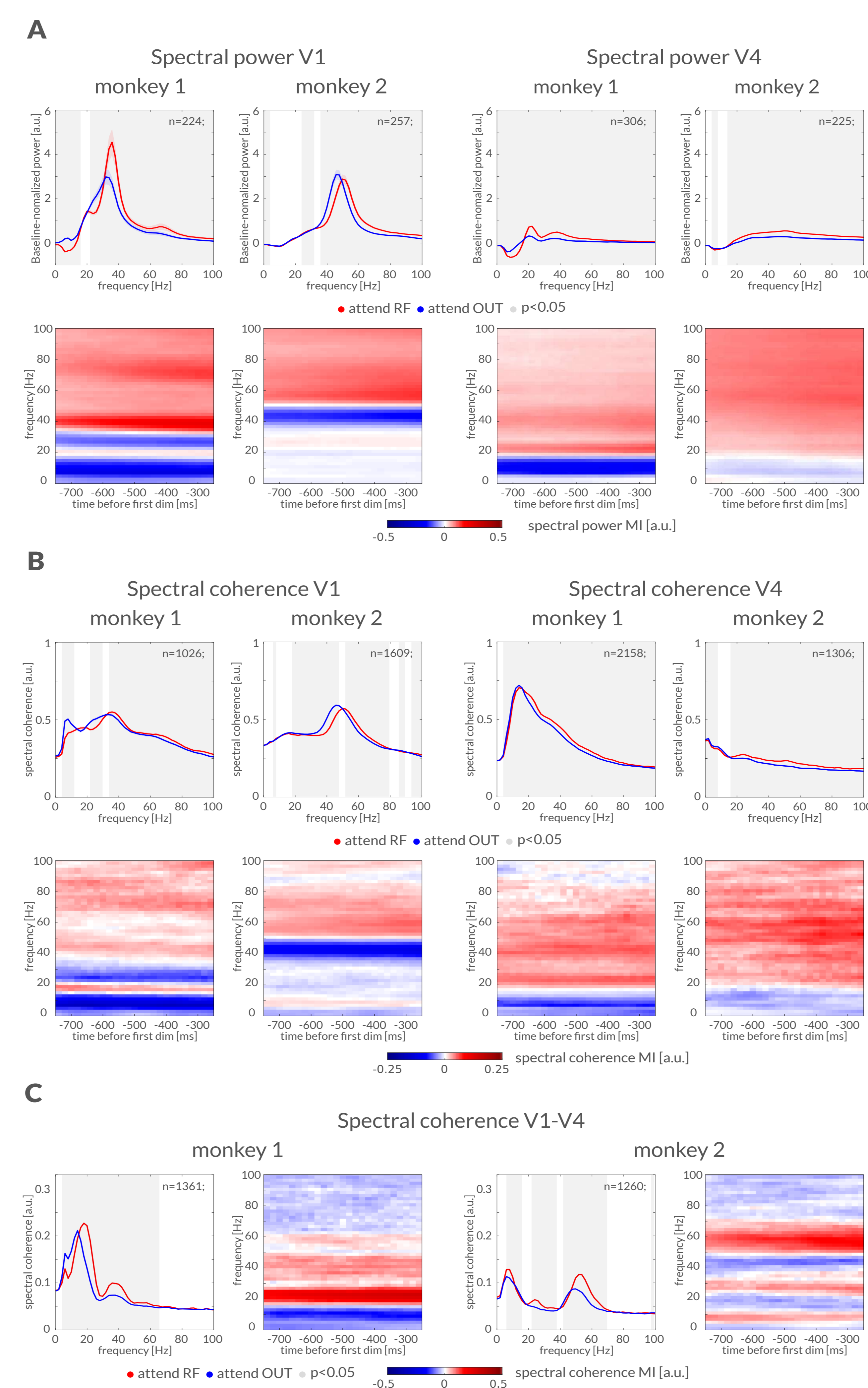
A) Visual cortical areas recorded; B) Laminar electrode probe visualization and laminar compartment assignment (supragranular, granular, infragranular) for LFP and MUA signals at different depths. Distances from laminar reference used for assignment: V1 infrag. -0.75±0.25 [mm], V1 granular -0.25±0.25 [mm], V1 suprag. 0.25±1 [mm], V4 infrag. -0.75±0.1 [mm], V4 granular -0.1±0.1 [mm], V4 suprag. 0.1±1 [mm]; C) Receptive Field maps (mean across depths) respectively recorded from V1 sites (left) and from V4 sites (right); D) LFP Current Source Densities across V1 depths (left) and V4 depths (right); B–D) Data are from a sample session simultaneously covering V1 and V4 in monkey 1.

## Figure 2 – Behavioral task



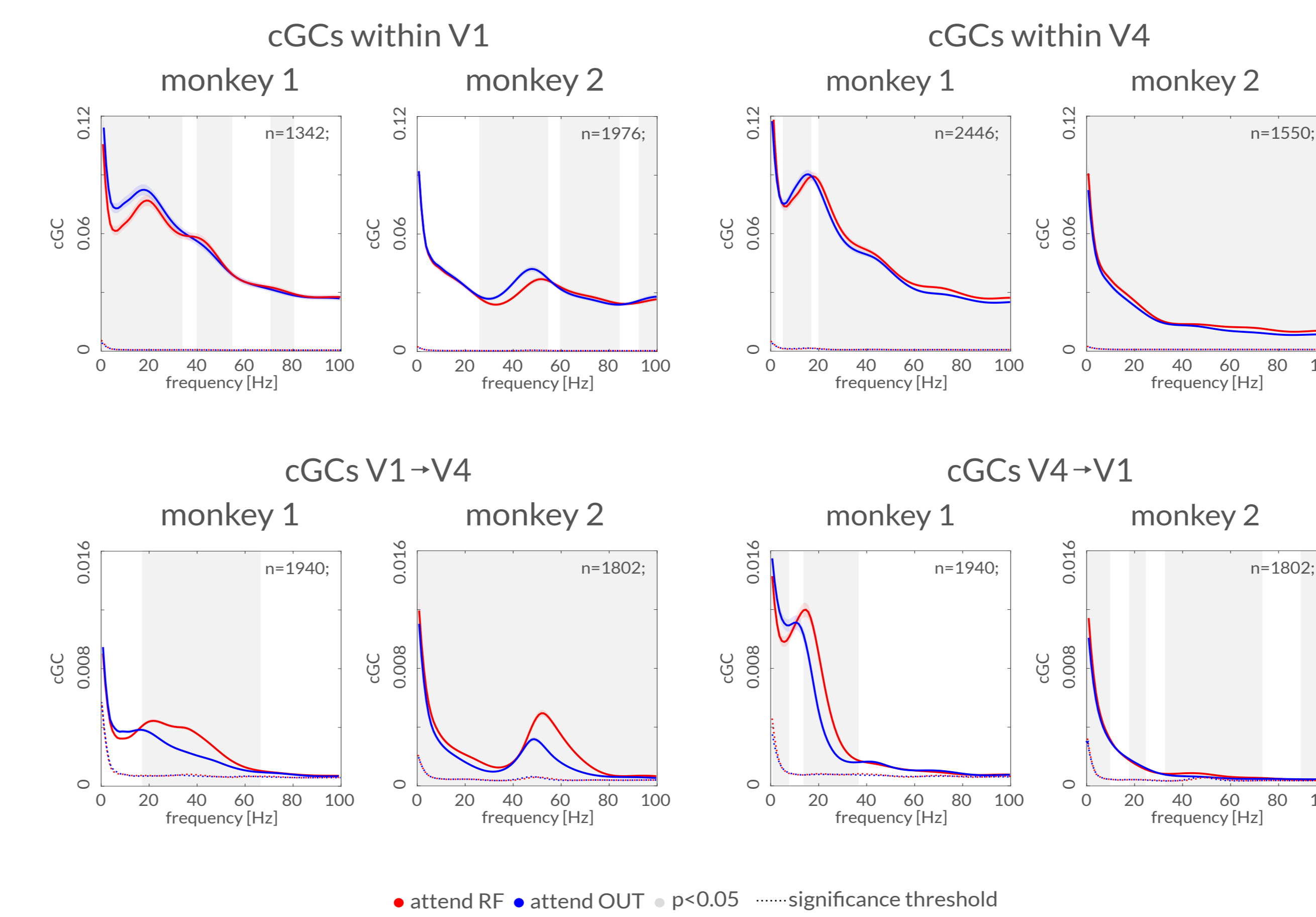
Covert, feature-based spatial attention task. The monkey holds the touch bar and fixates at Fixation Point (FP). Colored, moving grating stimuli appear at locations: RF, OUT<sub>1</sub> and OUT<sub>2</sub>. After a random delay, the attentional cue is presented at FP. At subsequent random delays, the colored stimuli sequentially dim. When cued stimulus dims, the monkey is asked to release the touch bar to receive fluid reward.

## Figure 3 – Spectral Analysis of LFPs



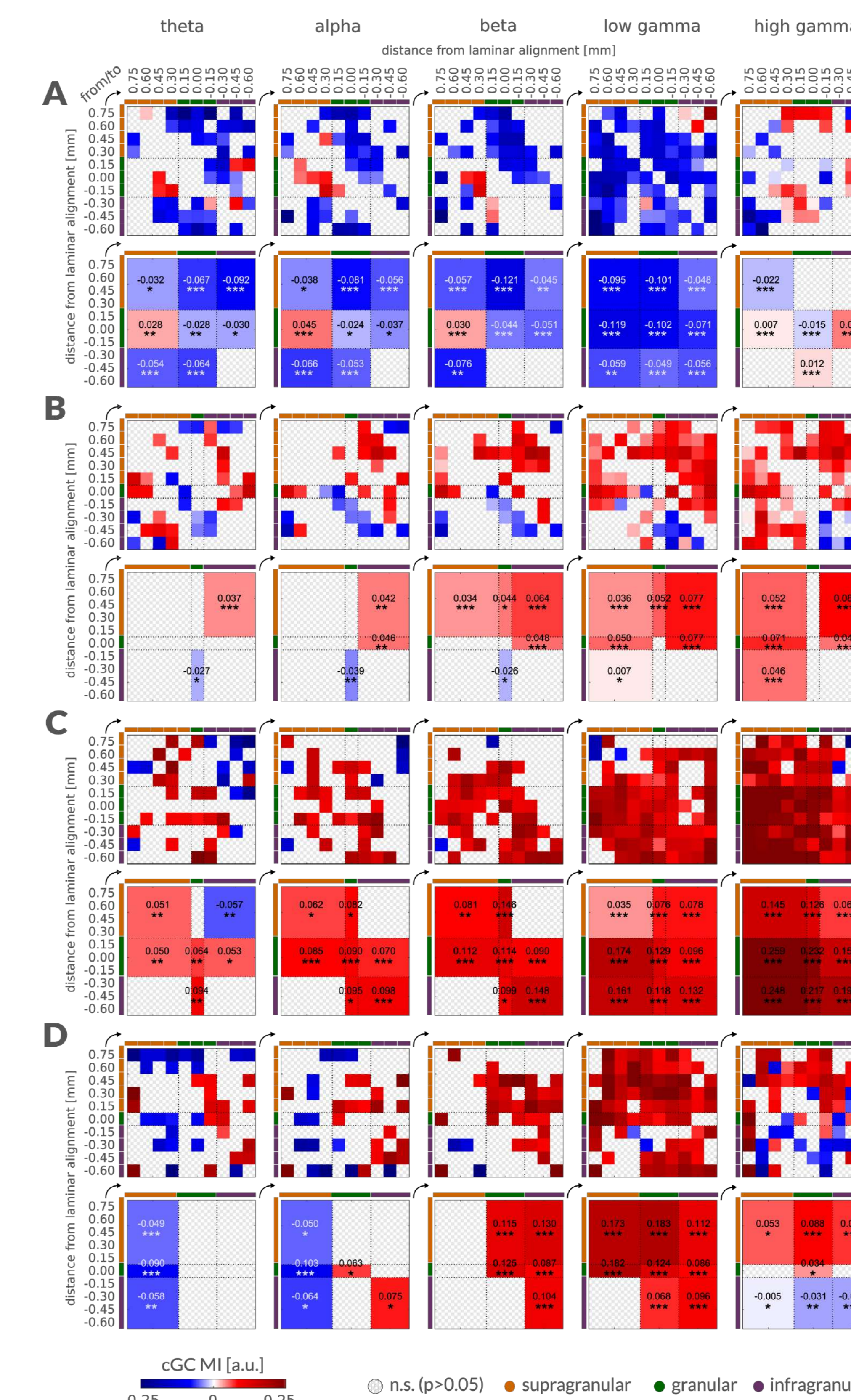
A) Spectral power (top row, mean ± sem) for a 500 ms time window before first dimming. Shaded gray background is for significant differences between attentional conditions ( $p < 0.05$ , Wilcoxon signed-rank tests, FDR corrected); Spectral power MI (bottom row, mean) for 500 ms time windows sliding in time with step 20 ms up to 1000 ms before the time of first dimming. B) Same as in (A), but for spectral coherence (top row, mean ± sem) and spectral coherence MI (bottom row, mean) averaged across depth pairs within V1 and within V4 columns. C) Same as in (A) but for spectral coherence (first and third panel from left, mean ± sem) and spectral coherence MI (second and fourth panel from left) between V1 and V4. A–E) LFP signals for the two monkeys are pooled across sessions and depths.

## Figure 4 – Granger causality magnitude



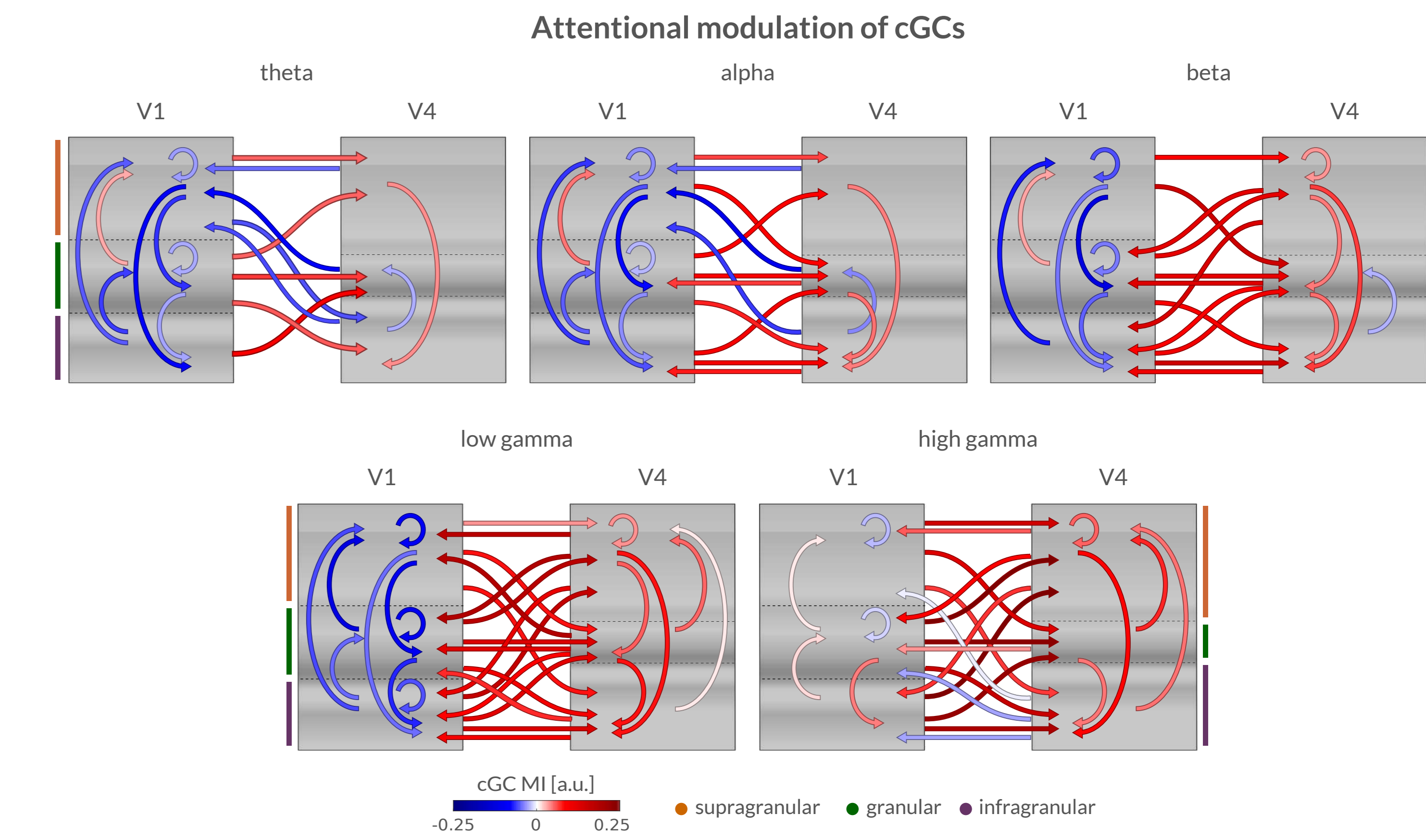
Conditional Granger Causality (cGC, mean ± sem) in frequency domain for intra-areal (within V1, within V4) and inter-areal (from V1 to V4, from V4 to V1) directed interactions among LFP signals at multiple depths, for the two monkeys. In any of the panels, significant difference between attentional conditions is reported as shaded gray background, and significance threshold for cGCs in both attentional conditions is reported as dotted line.

## Figure 5 – Granger causality attentional modulation



A) Attentional modulation of cGCs within V1 depths measured as MI for different frequency bands. Results are shown both at the level of single-channel interactions (top row) and pooled by laminar compartments (bottom row). B) Same as in (A) but for cGCs within V4. C) Same as in (A) but for cGCs from V1 to V4. D) Same as in (A) but for cGCs from V4 to V1. A–D) The values of cGC MIs are pooled between the two monkeys and assessed for statistical significance by Wilcoxon signed-rank tests, FDR corrected.

## Figure 6 – Summary



Graphical summary of results for cGC attentional modulation. Significant cGC MIs within V1 depths, within V4 depths and directed from V1 to V4, and from V1 to V4, pooled across monkeys. Statistical significance of MIs was assessed by Wilcoxon signed-rank tests, FDR corrected.

## CONCLUSIONS

- Attention induced changes of Granger causal interactions (GCI) often violated predictions related to frequency specificity of feed-forward and feed-back interactions [1,4].
- Within V1, attention increased granular to supragranular efficacy in low and mid frequency bands, reducing most other interactions.
- Within V4, attention mostly increased GCIs in a 'downwards' direction within the column, across all frequency bands.
- V1–V4 CGIs generally increased with attention between most compartments for most frequencies. This increase was most prominent in the gamma frequency range.
- V4–V1 CGIs were decreased in low frequency bands in an upward direction.
- V4–V1 CGIs increased across directions in the low gamma frequency range.

## REFERENCES

- [1] T. van Kerkoerle, M. W. Self, B. Dagnino, M. A. Gariel-Mathis, J. Poort, C. van der Togt, and P. R. Roelfsema, *Proc. Natl. Acad. Sci. USA* 111,14332 (2014).
- [2] T. van Kerkoerle, M. W. Self, and P. R. Roelfsema, *Nature Communications* 8, 13804 (2017).
- [3] A. S. Nandy, J. J. Nassi, and J. H. Reynolds, *Neuron* 93, 235 (2017).
- [4] A. M. Bastos, J. Vezoli, C. A. Bosman, J. M. Schoffelen, R. Oostenveld, J. R. Dowdall, P. De Weerd, H. Kennedy, and P. Fries, *Neuron* 85, 390 (2015).
- [5] D. Marinazzo, M. Pellicoro, and S. Stramaglia, *Computational and mathematical methods in medicine* (2012).